VF-840829--3

CONF-840829--3

DE85 001256

FORWARD ELECTRON PRODUCTION IN HEAVY ION-ATOM AND ION-SOLID COLLISIONS*

Ivan A. Sellin
University of Tennessee, Knoxville, TN 37996
and
Oak Ridge National Laboratory, Oak Ridge, TN 37831

Introduction †

A sharp cusp in the velocity spectrum of electrons, ejected in ion-atom and ion-solid collisions, is observed when the ejected electron velocity $\vec{v}_e$ matches that of the emergent ion $\vec{v}_p$ in both speed and direction. In ion-atom collisions, the electrons originate from capture to low-lying, projectile-centered continuum states (ECC) for fast bare or nearly bare projectiles, and from loss to those low-lying continuum states (ELC) when loosely bound projectile electrons are available. Most investigators now agr that ECC cusps are strongly skewed /1/ toward lower velocities, and exhibit full widths half maxima roughly proportional to v_p (neglecting target-shell effects, which are sometimes strong). Fig. 1 provides an example, comparing ECC & ELC cusp shapes. A close examination of recent ELC data shows that ELC cusps are instead nearly symmetric, with widths nearly independent on v_p in the velocity range 6 - 18 a.u., a result only recently predicted by theory. "Convoy" electron cusps produced in heavy ion-solid collisions at MeV/u energies exhibit approximately velocity-independent widths very similar to ELC cusp widths. While the shape of the convoy peaks is approximately independent of projectile Z, velocity, and of target material, it is found that the yields in poly-crystalline targets exhibit a strong dependence on projectile Z and velocity. While attempts have been made to link convoy electron production to binary ECC or ELC processes, sometimes at the last layer, or alternatively to a solid-state wake-riding model, our measured dependences of cusp shape and yield on projectile charge state and energy are inconsistent with the predictions of available theories.

†A more detailed discussion of similar topics, on a level more appropriate for specialists in ion-atom collision physics, will be given at the Debrecen satellite meeting on ion-atom collision physics, August 27-28, 1984. Recent work at Centro Atomico Bariloche, and at the Unversity of Aarhus will also be discussed in more detail in that same specialized paper.

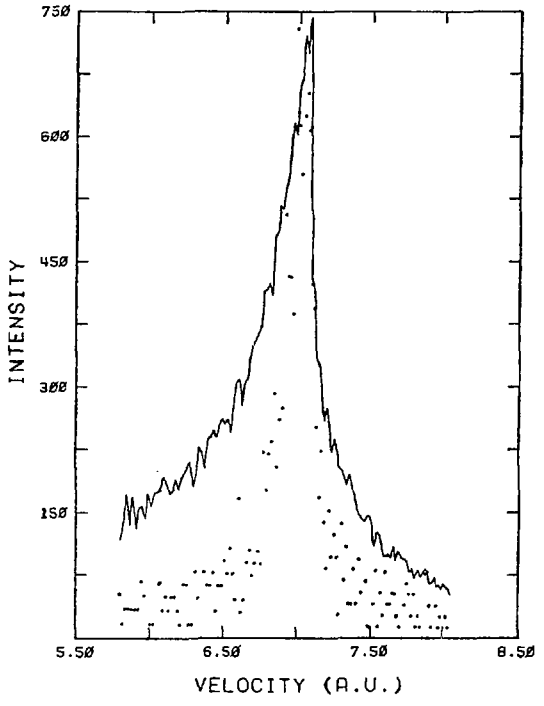

Fig. 1. Cusp for 20-MeV O^{7+} projectiles on Ar obtained in coincidence with O^{8+} (dots), overlaid with cusp containing all electrons not detected in coincidence with O^{8+} (solid line). The former is an ELC spectrum while the later represents an ECC spectrum. Differences in ELC and ECC cusp shapes are obvious.

When coincidence with emergent ion charge state q_e is required, ECC cusps can be sorted as to whether 0,1,2... additional bound-state captures occurred during the same collision which generated the continuum electron. Similarly, ELC cusps can be sorted as to how many additional electrons were lost. The shapes observed are relatively independent of whether or not additional capture or loss events occurred. The yields (production cross sections) tend to mimic the beam velocity, projectile Z, and projectile charge q dependence of corresponding single- and multiple-electron bound state capture and loss cross sections.

For convoy electron production in solids, cusp shapes are again found to be independent of q_e. More remarkably, for polycrystalline and randomly oriented monocrystalline targets, the yields are found to be nearly independent of q_e, i.e., to mirror the unweighted statistical fraction of emergent ions of each charge state, even though there is an appreciable projectile Z dependence, and, until recently, reason to believe that the observed convoys originate in many cases at a depth well within one mean-free path for charge changing of the exit surface. For well-channeled ions, however, the convoy yield is strongly

suppressed, pointing to the necessity of close approach to an atomic string in the bulk as a necessary precursor of convoy production.

Electron capture to the continuum (ECC)

Electron capture to the continuum describes capture to projectile-centered states, where the capture proceeds in analogy to electron transfer to bound states, but the wave function which describes the motion of the electron after collision is instead a projectile-centered continuum wave function. The phenomenon therefore represents a form of ionization, but one in which, for example, a plane-wave description of the captured electron is completely inappropriate. Rather, Coulomb waves centered on the projectile become a more appropriate description. Joseph Macek, in a series of publications with Eugene Rudd and others dating back to 1970 /2/ makes the following analogy. Ionization can be thought of as the natural continuation of excitation to a sequence of orbits of ever-increasing principal quantum number into the continuum. The excitation cross sections continue smoothly right through the ionization limit, provided an appropriate normalization of continuum states vis-a-vis excitation to high-n Rydberg states per unit bandwidth ΔE is considered. In like fashion, one may envision electron-capture events accompanying on ion-atom encounter into a sequence of orbits of ever-increasing principal quantum number n, whose production rate also continues smoothly from the region of high Rydberg states just below the continuum into the continuum. Somehow, this process went experimentally undiscovered and theoretically neglected during the 50-odd years which have elapsed since the initial development of the quantum theory. Although quantum mechnical theories of excitation, ionization, and capture to bound states were worked out in the 1920's and 1930's, the electron-capture contribution to ionzation was somehow ignored. That it can sometimes be extremely important is illustrated by a 1978 paper by Shakeshaft /3/ who finds that for certain energies (~40 keV), more than half the total cross section for ionization of hydrogen by protons is accounted for by this process.

The generally accepted form of the cross section for production of electrons ejected in the forward direction with velocities close to that of the incident ion is given by

$$\frac{d\sigma}{d\vec{v}} \propto \frac{f(v_e, v_p, \theta_e)}{|\vec{v}_e - \vec{v}_p|} , \qquad (1)$$

where $f(v_e, v_p, \theta_e)$ is finite for $\vec{v}_e = \vec{v}_p$. $\vec{v}_e$ and $\vec{v}_p$ refer to the laboratory frame electron and and projectile velocities. The denominator of Eq. (1), symmetric about $\vec{v}_e = \vec{v}_p$, gives rise to the "cusp" shape and

results from the Coulomb interaction between the outgoing projectile ion and the ejected electron. The function $f(v_e, v_p, \theta_e)$ can incorporate the observed asymmetry, and as in Ref. 4 we expand it in terms of a projectile frame "partial-wave" expansion,

$$f(v_e, v_p, \theta_e) = \tfrac{1}{2}(\pi)^{-\frac{1}{2}} \sum_{\ell} (2\ell+1)^{\frac{1}{2}} a_\ell P_\ell(\cos\theta_e') \quad . \tag{2}$$

Note that this is a partial wave expansion of the cross section and not that of a wave function amplitude as is more commonly the case. The coefficients a_ℓ are now functions only of v_e and v_p (for given ion and target Z), and since $v_e' = |\vec{v}_e - \vec{v}_p|$ is small in the neighborhood of the cusp peak, the a_ℓ may be expanded in a Taylor series in v_e', resulting in

$$\frac{d\sigma}{d\vec{v}_{e}'} = \frac{C}{v_e'} \sum_{n,\ell} B_{n,\ell}(v_p) (v_e')^n P_\ell(\cos\theta_e') \quad , \tag{3}$$

where $B_{00} \equiv 1$.

To compare the cross section with the measured distributions $Q(v_e, \theta_e)$, the product of the spectrometer acceptance function $S(v_e, \Omega_e)$ and the cross section $d^2\sigma/dv_e\, d\Omega_e = (v_e)^2 (d\sigma/d\vec{v})$ are integrated over the experimental acceptances in velocity and angle, resulting in

$$Q(v_e, \theta_e) = C \sum_{n,\ell} B_{n,\ell}(v_p) \int_{v_e} \int_{\Omega_e} (v_e)^2 (v_e')^{n-1} P_\ell(\cos\theta_e') \, S(v_e, \Omega_e) dv_e \, d\Omega_e \quad . \tag{4}$$

We now summarize results from a number of our most recent experiments in ECC,/5/ obtained under the leadership of Scott D. Berry. To determine the best fit values of $B_{n\ell}$ for the cross section expansion given in Equation (3), the value of Equation (4) was calculated for trial values of the coefficients ($B_{n\ell}$) and the angle θ_0, and the resulting function was fitted to the experimental data distributions using a least squares fitting procedure. Good agreement (within 5%) with values of θ_0 estimated from geometrical calculations was always obtained. Only those coefficients with n = 0, 1 and ℓ = 0, 1, and 2 were needed for the fits to converge to their approximate best fit conditions. In Figure 2, the terms of Equation (4) for a given coefficient are displayed for comparison with all amplitudes $B_{n\ell}$ set to 1 and a delta function lineshape $R(v_e)$; the terms corresponding to ℓ = 0, 1, and 2 are labeled (solely for convenience) S_n, P_n, and D_n respectively.

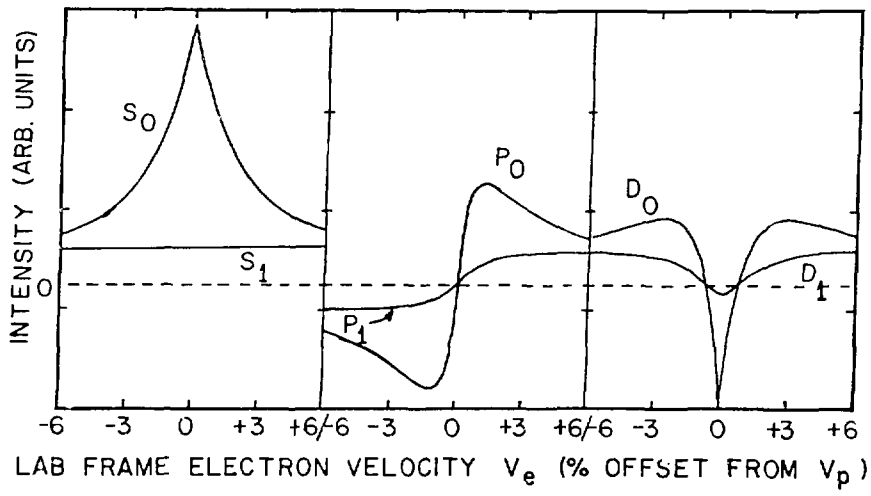

Fig. 2. Examples of the cusp shape contributions from the six lowest order terms of the cross section expansion used to characterize the laboratory frame ECC cusp shape. These are displayed for normalized amplitudes $B_n = +1$. Values of $\theta_o = 1.4°$ and a δ-function R (v_e) velocity line width were assumed for the analyzer parameters here. The velocity scale is represented in terms of the percentage difference between the lab frame electron and projectile velocities.

In Table I a summary of numerical results of the fitting procedure for] various combinations of projectile and target species is presented. Within parentheses beside values for each $B_{n\ell}$ one standard deviation variances are listed for those cases in which the amount of data permitted fits to multiple data sets; in all other cases best fit results were found by summing all data into a single spectrum for fitting.

The most striking feature of the results presented in Table I is the remarkable consistency of the values found for the major asymmetric term P_o, for the wide variety of target and projectile combinations used in these experiments ($8 \leq Z_p \leq 18$; $Z_t = 1,2$; $6 \leq v_p \leq 18$). The S_1 term shows a large percentage variation in values found from the fitting procedure, but the effect on the overall shape is minor, because of the size of this term compared to the dominant S_o term, especially at the cusp peak. This variation is most likely caused by errors in background subtraction, the accuracy of which was sensitive to slight variations in beam steering conditions. The D term values found in all cases are also small, and are mainly important to the fit in the wings of the cusp where $v_e' << 1$ is not as valid.

TABLE I Results of fits for several targets and projectiles. The coefficients are explained in the text; the coefficient for the dominent S_0 component is normalized to 1. Errors (in parentheses) where given are 1 standard deviation derived from multiple fits.

Projectile	Target	Velocity	Fit Angle	S_1	P_0	P_1	D_0	D_1	χ^2
C	H	6.3 a.u.	2.14°	.32	-.42	-.37	-.03	-.21	4.94
	H_2		1.97	-.20	-.48	-.08	-.07	.01	1.09
O	He	8.6	1.83	.23	-.25	-.40	-.25	.07	1.23
		10.0	1.73	-.17	-.37	-.05	-.06	-.05	4.29
		15.4	1.41	.22	-.49	-.04	-.03	.00	1.63
				(.11)	(.03)	(.01)	(.03)	(.02)	(.24)
		16.6	1.40	.08	-.47	-.05	.10	.12	1.23
				(.19)	(.04)	(.08)	(.10)	(.10)	(.34)
		17.2	1.40	.02	-.48	-.02	.03	.02	1.30
Ne	He	17.6	1.65	.01	-.47	-.02	.02	----	1.49
				(.01)	(.03)	(.01)	(.01)		(.22)
Ar	He	15.0	1.45	.57	-.39	-.26	-.17	----	1.0
		18.1	1.41	.43	-.47	-.12	-.17	----	1.4

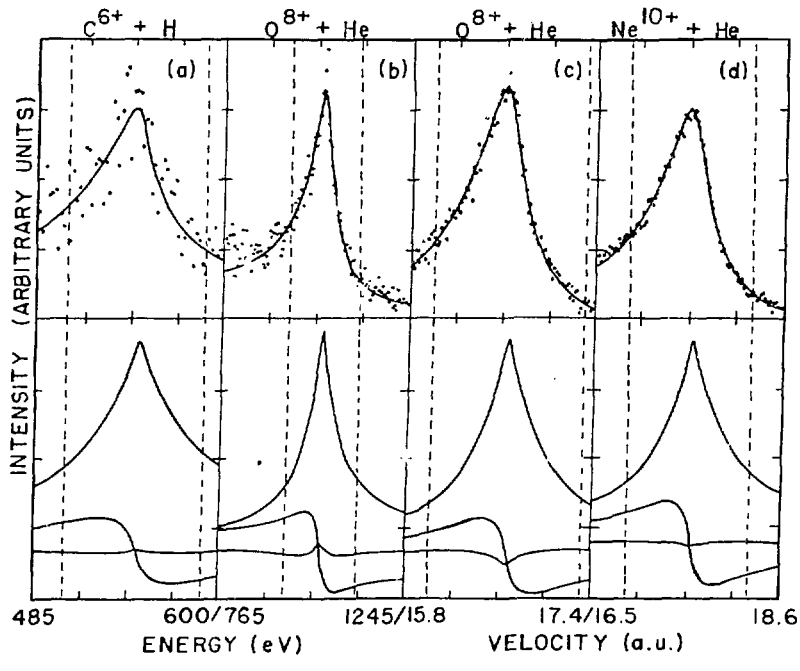

Fig. 3. The top row shows four comparisons between fitted spectra (solid lines) and data (dots) incorporating background subtraction where appropriate for: (a) 12 MeV bare carbon projectiles, (b) 30 MeV and (c) 110 MeV bare oxygen projectiles, and (d) 155 MeV bare neon projectiles. The vertical dashed lines indicate equivalent arbitrary $(1\pm.04)v_p$ limits for each of four spectra. The bottom row displays S, P, and D components of the fitted function (summed over both n = 0, 1 components) for the corresponding fitted function shown above. The bottom spectra have been displayed with a δ-function linewidth, to remove the dependence of the cusp shape on the particular experimental line width, allowing for a more direct comparison of the results.

In Figure 3, we present representative fit results for helium targets, as well as that for atomic hydrogen (the contribution of molecular targets has been subtracted), and the resulting S, P, and D component parts of each fit. The similarity of the cusp shape for both helium and hydrogen targets suggests that at least for the velocities considered here the results for helium targets approximate those for atomic hydrogen targets at a satisfactory level.

We hope that by presenting our results in the above model-independent manner, which attempts to account for the variations in experimental arrangements, further theoretical investigation into the shape of the ECC cusp will be stimulated, especially concerning the detailed dependence of the asymmetry on Z_p, Z_t, and v_p observed. In particular, the promising approach of Jakubassa-Amundsen /6/ in explicating our argon projectile data /7/ may warrant

application of her method to the combinations of projectile Z and v discussed here. Also, it is our expectation that by making further systematic studies of the cusp shape, especially as a function of collection angle, and through a similar method of analysis, more insight into the nature of the ECC cusp asymmetry and its theoretical explanation will be possible.

Electron loss to the continuum (ELC)

When partially ionized projectiles undergo atomic collisions, it is now well known /1,8/ that a superficially similar peak in the velocity spectrum of electrons emitted in the forward direction arises from projectile ionization, and that cross sections for ELC dominate whenever loosely bound projectile electrons are available. Though the "C" in ELC may seem redundant, its use reminds us of parallel ECC phenomena and further reminds us that electron loss from heavy particles (usually targets) can occur through electron capture by the binary collision partner, thereby liberating no electrons into the continuum.

Recent experiments /9/ have measured the shape of the ELC cusp, characterized by the width [full width at half maximum (FWHM)], the forward-backward asyummetry with respect to the cusp peak, and the total cusp cross section integrated over an arbitrarily chosen interval

$$(v_p - 0.5 \leq v_p \leq v_p + 0.5).$$

For highly charged projectiles having relatively loosely bound L-shell electrons, we have found an almost symmetric cusp with a narrow width in the range $\Delta = 0.25$–0.3 a.u. nearly independent of v_p, Z_p, and the target. These results differ significantly from corresponding findings for ECC and adequate theoretical explanation had heretofore not been available. A direct comparison with the calculation for the 1s state /8/ is not possible for two reasons: In any experiment which does not detect the final charge state of the outgoing projectile in coincidence, the ELC contribution dominates the cusp only if sufficient loosely bound n=2 electrons are available. Furthermore, the Born criterion $Ze^2/nv \ll 1$ is in most cases studied to date only marginally satisfied for the deeply bound 1s state. A systematic theoretical study of the ELC cusp shape as a function of the initial state of the released electron, its binding energy, the projectile velocity, and the target structure was therefore initiated.

Previous calculations of Briggs, Dreper and Day /8/ for ionization of the 1s state in the low-velocity limit nas been generalized by Burgdörfer /8/ to arbitrary hydrogenic initial states $|nlm\rangle$ by evaluating the bound-free transition form factor using a group-theoretical method. In the paper by Burgdörfer et al. an algebraic treatment of Coulomb excitation was extended to a calculation of the bound-free transition form factor for low-lying continuum states, exploiting the continuity across the ionization limit. The

low-velocity limit of the continuum wave function was examined as a coherent superposition of parabolic Rydberg states $|n',n'_1,n'_2m'>$, incorporating the boundary conditions for an incoming (outgoing) Coulomb wave. This result was then used to calculate the bound-free transition form factor as a Rydberg limit $n'\to\infty$ of the bound-bound transition form factor. Numerical results for the doubly differential cross-section (DDCS) and the cusp shape were then compared with recent experimental data for ELC from our laboratory.

Quantitative comparison with our experimental results can be expected to be possible only if: (a) the projectile velocity is large compared to the orbital velocity of the released electron; (b) the initial state can be approximated by a hydrogenic wave function without serious error; and (c) additional charge-transfer contributions (ECC) can be neglected. Most of the data taken so far for highly charged projectiles in our laboratory satisfy these requirements only marginally. An exception are these cusp data for O^{5+}. The large electron-loss cross section for the loosely bound 2s electron permits an almost "pure" ELC measurement without a significant ECC contribution, and without the need for performing a coincidence experiment. The 2s state of the Li-like configuration can be described by a hydrogenic wave function with an effective charge $Z_{P,eff}=6.3$ to a reasonable degree of approximation. The deviation from the asymptotic charge seen by the ionized electron at large distances, $Z_{P,asym}\sim 6$, is only ~5%. For the experimental data in the region $7<v_p<12$ with $v_p/v_{orbital}>2$ the Born approximation provides a rough estimate for the ELC cross section.

Figure 4 displays the ELC cusp width for O^{5+} on argon. The calculation includes, besides the dominant 2s cross section (~90%), the smaller contributions of the two 1s electrons (~10%) also described by hydrogenic orbitals with the Slater value $z_{P,eff}=7.65$. The linewidth is found to be much smaller than predicted for an isotropic cusp, also shown in Fig. 4, and in good agreement with our data. This result strongly emphasizes the importance of the large transverse anisotropy as a source of the narrowing and of the weak v_p dependence of Γ observed in ELC experiments for few-electron projectiles. Further comparisons for the "total" cusp cross section σ^{ELC} as determined by integration of $d\sigma/dv_e$ between $v_p-0.5$ and $v_p+0.5$ are also discussed in Ref. 8.

One of the most interesting of Burgdörfer's recent findings is that for selected nlm states, the customarily observed cusp not only can take on a very different shape -- it can even appear inverted! Figures 5 and 6 display $d\sigma/dv$ for He on H at 10 au and 4 au, repectively. A striking inversion in the cusp, producing a valley in the observed spectrum of ionization electron, is seen for the $2p_o$ initial state of the projectile. Such a structure has not yet been observed experimentally.

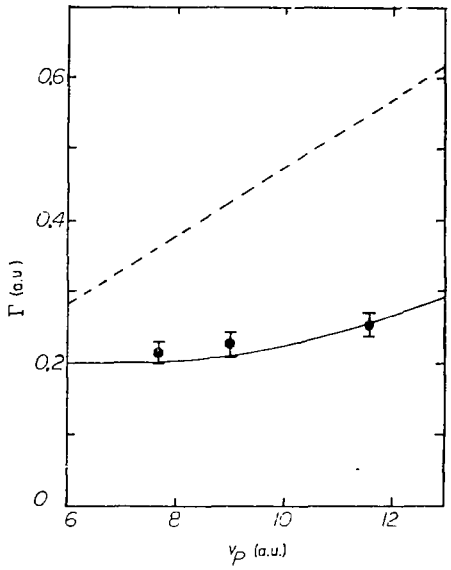

Fig. 4. ELC cusp width for O^5 on argon ($\theta = 3.14 \times 10^{-2}$ rad~1.8°) as a function of the projectile velocity; —, Reference 8; — — —, width for isotropic electron emission; ⧫ experimental data.

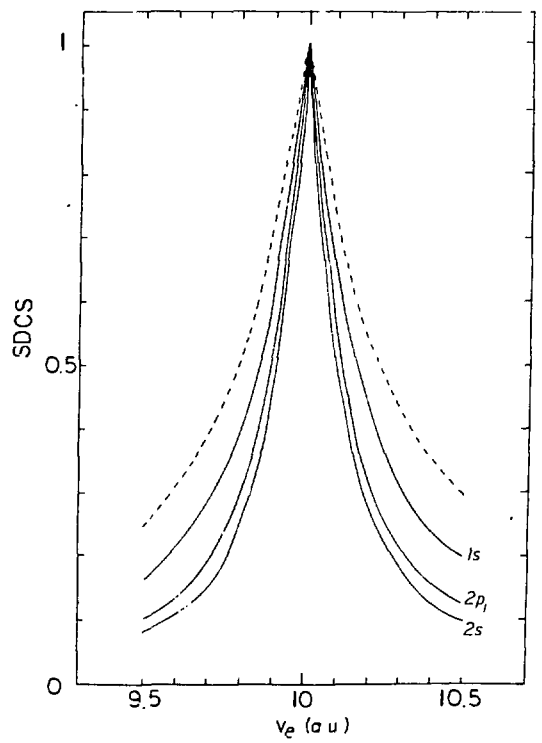

Fig. 5. Normalized singly differential cross section $d\sigma/dv_e$ for ELC of $He^+(n,l,m)$ on H at $v_P = 10$ a.u. ($\theta_0 = 3 \times 10^{-2}$ rad); — — —, cusp shape for isotropic electron emission.

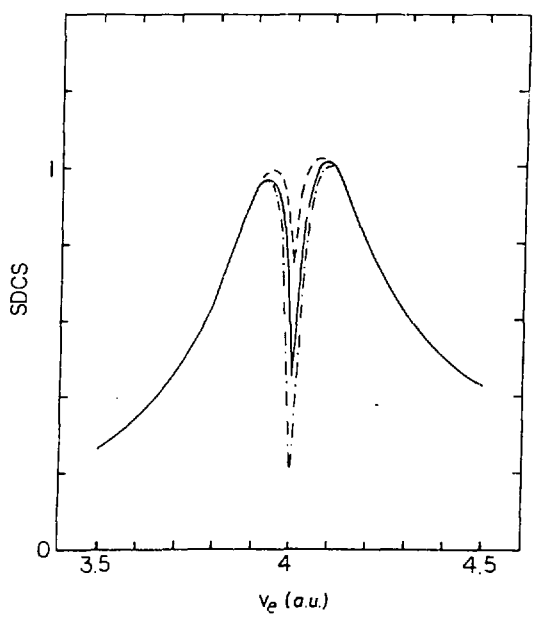

Fig. 6. Cusp inversion for ELC of $He^+(2p_0)$ at $v_P = 4$ a.u. ($\theta_0 = 3 \times 10^{-2}$ rad) and different targets: ——, hydrogen; — — —, helium; —·—, argon.

It is interesting to note the similarities and differences of the forward-backward asymmetry for ECC and ELC. As in the case of ECC we find that the asymetry of the DDCS is a signature of the presence of higher-order Born terms. There is, however, a remarkable difference: In the limit of asymptotic projectile velocities $v_p >> 1$ the DDCS asymmetry persists for ECC because of the dominance of the second-order Born contribution, whereas for ELC the DDCS should become symmetric because the first order Born approximation is believed to be the leading term of the perturbation expansion for large v_p.

A central feature of the recent calculation performed by Burgdörfer /8/ is that the narrow ELC cusps, with widths approximately independent of collision velocity, are a consequence of preferential transverse electron emission from the 2s level in 3- and 4-electron ions, coupled with convolution over the narrow range of observation angles admitted in most ELC experiments. If the DDCS in the projectile frame is expanded in multipoles as is usual for anisotropic emission, it can be parameterized as

$$do/dv = a_0[1 + \beta_2 P_2(\cos\theta) + \beta_4 P_4(\cos\theta)],$$

where the emission velocity v and polar angle θ are expressed in the projectile frame, P_2 and P_4 are Legendre polynomials, a_0 sets the isotropic emission level, and the second and fourth order coefficients β_2 and β_4 determine the degree and nature of the anisotropic component of emission. Various symmetry considerations prohibit other multipoles in the expansion of the DDCS for pure ELC processes. For the projectiles (O^{5+}) targets (He, Ar), and velocities we have recently studied, $\beta_2 \sim -0.6$ and $\beta_4 \sim +0.1$, which leads to an emission pattern which is strongly transverse to the ion beam. Our preliminary measurements of the emission distribution exhibit definite transverse anisotropy.

Figure 7 displays a sample ELC cusp for O^{5+} on Ar obtained by Elston et al./10/ using a position sensitive detector with a spherical sector spectrometer to provide angle-resolved emission spectroscopy.

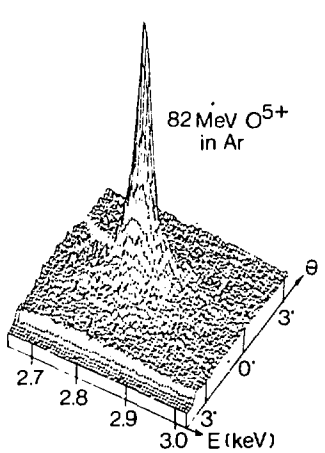

In Figure 8 plots of contours of equal intensity as observed in the laboratory frame for 82 MeV O^{5+} on He and Ar targets are compared with the

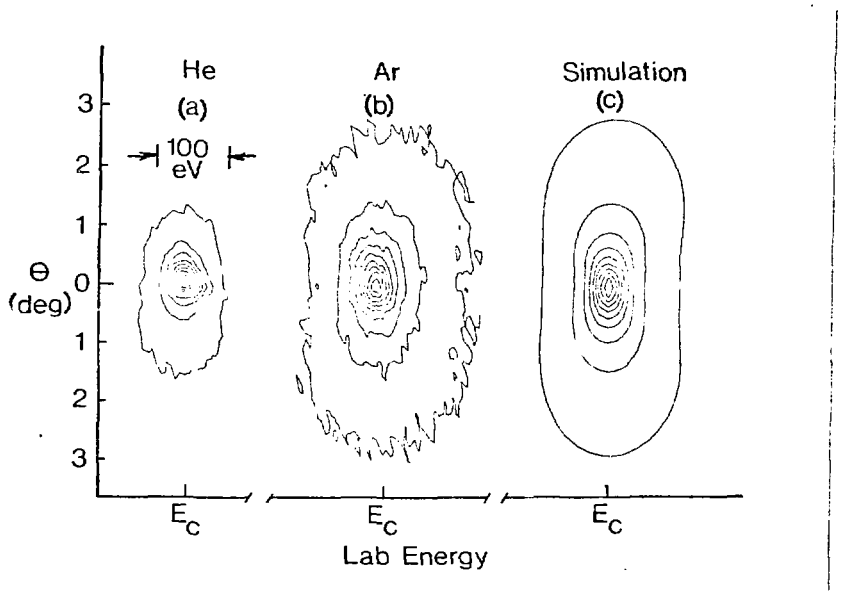

results of a simulation based on the asymmetry parameters quoted above and upon a convolution with the instrumental response function we expect from essentially geometric considerations. Corrections for the transformation between projectile and laboratory frame and spectrometer transmission efficiency are also included. It is seen that the degree of asymmetry exhibited by the data away from the central portion of the cusp (where the singular nature of the cusp results in extreme sensitivity to the details of the instrumental response function) is reasonably good. The cusps obtained with argon targets are a bit narrower than the simulated data, and the helium cusps are significantly narrower overall than expected, a puzzling result if one expects the calculations to be more reliable for a simpler target.

Zero-degree Auger Electron Spectrometry

The analysis of electrons emitted into the forward direction also permits the study of doubly excited, high Rydberg autoionizing states, where low Auger energies (e.g. 2-20eV) can be very conveniently detected. For Be-like ions excited in gas or foil targets, there is a high probability for simultaneous excitation of two electrons to bound states (one high lying). The advantages of high beam velocity combined with observation at zero degrees are: 1) minimizing of Doppler spread at zero degrees; and 2) kinematic shifting of very low energy Auger transitions to convenient laboratory frame energies. As

this very interesting subject lies outside the principal scope of this paper, interested persons may consult ref. 9 for further details.

Acknowledgements

Thanks are due numerous colleagues and collaborators who have participated in work in our laboratory, most of whom are identified in the references. In our most recent experiments, especially valuable contributions have been made by my faculty colleagues Stuart B. Elston, Marianne Breinig, and Joachim Burgdörfer; and by graduate research assistants Scott D. Berry and Gary A. Glass. Quintessential contributions to our earliest experiments in this field were made by Charles R. Vane and Martin Suter. We are most grateful as well to K.-O. Groeneveld and colleagues of the University of Frankfurt/M for joint experiments carried out at GSI-Darmstadt; to N. Stolterfoht, H. Schmidt-Böcking, and colleagues for those at the Hahn-Meitner Institute, Berlin; to R. Marrus and H. Gould for those at the LBL SuperHILAC; and to R. Laubert for those carried out at the BNL tandem laboratory. We thank the staffs of the ORNL tandem and Holifield Heavy Ion Research Facilities; of the LBL SuperHILAC; of GSI; and of HMI-VICKSI for their invaluable assistance in our use of their excellent accelerator facilities, without which the work discussed would not have been possible.

* This research was supported in part by the National Science Foundation; the U. S. Department of Energy, under contract no. DE-AC05-84OR21400 with Martin Marietta Energy Systems, Inc.; and DFG and BMFT in West Germany. The results pertaining to hydrogen targets were supported by the Fundamental Interactions Branch, Division of Chemical Sciences, Office of Basic Energy Sciences, of the U. S. Department of Energy, under contract DOE DE-AS05-79ER10512.

References

/1/ M. Breinig, et al., Phys. Rev. A25 (1982) 3015, and references quoted therein.

/2/ M.E. Rudd and J. Macek, Case Stud. At. Phys. 3 (1972) 125.

/3/ R. Shakeshaft, Phys. Rev. A 18 (1978) 1930.

/4/ W. Meckbach, I.B. Nemirovsky and C.R. Garibotti, Phys. Rev. A 24 (1981) 1793; M.W. Lucas, W. Steckelmacher, J. Macek, and J.E. Potter, J. Phys. B 13 (1980) 4833; J. Macek, J.E. Potter, M.M. Duncan, M.G. Menendez, M.W. Lucas, and W. Steckelmacher, Phys. Rev. Lett.46 (1981) 157.

/5/ S.D. Berry, G.A., Glass, I.A. Sellin, K.O. Groeneveld, D. Hofmann, L.H. Andersen, M. Breinig, S.B. Elston, P. Engar, and M.M. Schauer, N. Stolterfoht, N. Schmidt-Böcking, G. Nolte, and G. Schiwietz, Submitted for publication to Phys. Rev. A.

/6/ Jakubassa-Amundsen, J. Phys. B 16 (1983) 1767.

/7/ M. Breinig, S.B. Elston, I.A. Sellin, L. Liljeby, R. Thoe, C.R. Vane, H. Gould, R. Marrus and R. Laubert, Phys. Rev. Lett. 45 (1980) 1689.

/8/ J. Burgdörfer, M. Breinig, S.B. Elston, and I.A. Sellin, Phys. Rev. A 28 (1983) 3277 and references therein; J. Burgdörfer, Phys. Rev. Lett. 51 (1983) 374; F. Drepper and J.S. Briggs, Phys. B 9 (1976) 2063; J.S. Briggs and J.S. Drepper, ibid. 13 (1978) 4033; Briggs and Day, M.H. ibid. 13 (1980) 4794; M.H. Day, ibid. 13 (1980) L65; 14 (1981) 231.

/9/ M. Breinig, et al., Phys. Rev. A 25 (1982) 3034; S.B. Elston, Inner-Shell and X-Ray Physics of Atoms and Solids D.J. Fabian, H. Kleinpoppen, and L.M. Watson, eds. New York and London: Plenum Press (1980), 127.

/10/ S.B. Elston, Proceedings of the 12984 Symposium on the Physics of Electron Ejection in Ion-Atom and Ion-Solid Interactions, Aarhus, Denmark; Lecture Notes in Physics (Springer-Verlag) to be published.